

## Post-irradiation flashes and continuous emission from solid deuterium

J. A. Forrest and R. L. Brooks

*Guelph-Waterloo Program for Graduate Work in Physics, University of Guelph, Guelph, Ontario, Canada N1G 2W1*

(Received 18 July 1996)

Optical emission from proton-beam-irradiated solid deuterium near 800 nm has been studied after termination of the proton beam. The continuous red emission shows a residual intensity that persists over 30 min from termination of the beam. Optical flashes can also be thermally triggered over 10 min after termination of irradiation. Such triggered flashes are shown to quench the infrared absorption of Stark-shifted charge-induced features. Ultraviolet photons can stimulate this red emission after termination of irradiation with no measurable decrease in intensity for 40 min. The cause of this continuous emission and optical flashes is discussed in the light of these results. [S0163-1829(97)02802-6]

### I. INTRODUCTION

Irradiated solid hydrogens display a number of interesting spectral features not found in the unirradiated solid. The first evidence of such radiation-induced features was found by Souers *et al.*<sup>1</sup> in hydrogen mixtures containing tritium. These solids, when cooled below about 10 K, showed additional lines in the fundamental absorption spectrum. The new lines were interpreted as Stark-shifted single-molecule transitions. The Stark shifts were caused by the presence of trapped charges in the lattice, these charges being the net result of the ionizing tritium radioactivity.

Proton-irradiated samples also showed these features. This latter method, the one used in this study, allows the irradiation level to be easily varied, and also to be turned on and off, permitting the time dependence of the features to be studied. Thorough study of the timing behavior of these features led to a model of the dynamics of charged species in the solid.<sup>2</sup> This model involves two species of each charge, one mobile and one less mobile. Each of the less mobile charged species is responsible for induced absorption features. The mobile negative charge is thought to be a small polaron and its immobile counterpart an electron trapped in the form of a bubble. The mobile positively charged species is thought to be a  $D_3^+$  ion while the immobile positive species is a positive ion cluster of the form  $D_3^+(D_2)_n$  with  $n=3$  the most likely cluster.<sup>3,4</sup> All radiation-induced absorption features show a monotonic increase in intensity as the temperature is lowered below about 10 K, and are much weaker in  $H_2$  than in  $D_2$ .

In addition to the Stark-shifted features, a number of spectral features also attributed to trapped electrons have been observed in irradiated solid hydrogens. While most features are observed in all isotopes, we will restrict our attention here to deuterium, for which there are more numerous results. A broad infrared absorption, centered on  $1.7 \mu\text{m}$ , observed in the irradiated solid has been interpreted as the first bound-bound transition ( $1s-1p$ ) of the electron in its trap.<sup>5,6</sup> A broad absorption in the ultraviolet spectral region of irradiated  $D_2$ , centered on 330 nm, is similarly interpreted as the bound-free spectrum of the trapped electrons. A simple square-well model for the electron gives a good fit to the

observed spectrum for a well depth of  $3.8 \text{ eV}$ .<sup>3,7</sup> Stark-shift calculations for the infrared features, as well as models for the other electron bubble features, all lead to an electron bubble size of  $5.5 \pm 0.4 \text{ \AA}$ . These three independent experimental observations, all leading to approximately the same bubble size, make the existence of electron bubbles in the irradiated solid a convincing conclusion. A more thorough review of radiation-induced features in solid hydrogens can be found in Ref. 4.

The scenario which is thought to occur when ionizing radiation, such as protons, is incident on the sample is as follows. The proton beam ionizes  $D_2$  molecules to form  $D_2^+$  ions and energetic electrons. These electrons lose energy through inelastic scattering with host molecules and rapidly become thermalized. Simple classical calculations predict the electron to lose all of its excess energy in a matter of picoseconds. The resulting thermal electrons are the mobile small polaron species. The electron bubbles are thought to form when a small polaron becomes initially localized by lattice defects such as vacancies. The now localized electron has a large zero-point motion because of its small mass, and pushes the surrounding molecules away. By modeling the solid as a polarizable fluid, Bose and Poll<sup>8</sup> have examined the stability of this mechanism theoretically, and find bubbles formed in this manner to be stable for bubble radii of  $4.7 \text{ \AA}$ . Experiments on the mobility of charge carriers in solid hydrogens also support the idea of bubble formation. Meanwhile, the  $D_2^+$  ions rapidly convert to  $D_3^+$  and an atom of deuterium. The  $D_3^+$  moves about like a small polaron hole. If the  $D_3^+$  does not undergo dissociative recombination, it forms a cluster, probably  $D_9^+$ , which is highly immobile.

The atoms formed along with  $D_3^+$  have themselves been the subject of many electron-spin-resonance (ESR) experiments. Webeler measured a large concentration of atoms in solid  $H_2$  doped with tritium at temperatures below 1 K.<sup>9</sup> More recently, Miyazaki and Morikita have performed a number of ESR experiments on  $\gamma$ -irradiated samples from a  $^{60}\text{Co}$  source.<sup>10</sup> Collins *et al.* measured a sudden triggered energy release from tritium-doped solid deuterium and were able to correlate that to a sudden decrease in the atom concentration of their sample.<sup>11</sup> That much higher deuterium

atom concentrations can be supported in solid  $D_2$  than hydrogen atom concentration in solid  $H_2$  was reported by Iskovskikh *et al.*<sup>12</sup> and we have recently summarized this work.<sup>13</sup>

Emission from irradiated solid  $D_2$  has also recently been observed. The first such emission was reported by Stenum *et al.*<sup>14</sup> in electron-irradiated solid  $D_2$  films. This emission, centered near 270 nm, was interpreted as the  $nd^2E' \rightarrow 2p^2E'$  transition in  $D_3$ . Another emission, much more intense than the UV one above, in the near-infrared spectral region, has been observed in irradiated  $D_2$ . This emission was observed in tritium-doped, electron-irradiated, and proton-irradiated samples independently.<sup>15</sup> The infrared emission was observed at temperatures greater than 10 K, in contrast to previously observed radiation-induced spectral features. Brooks *et al.*<sup>13</sup> later showed that the emission persisted to even higher temperatures, becoming unobservable only after the solid had melted. This work also showed that the emission became substantially redshifted at higher temperatures.

Besides a continuous emission in the near-infrared spectral region, optical flashes, in which the intensity increases two to three orders of magnitude above the steady-state value for about 50 ms, have also been observed with nearly the same spectrum.<sup>16</sup> These flashes can occur spontaneously when the sample is irradiated at temperatures lower than 4.2 K or can be induced by subjecting the sample to a short heat pulse.<sup>17</sup> In this paper we shall show that they can also be induced over 10 min after irradiation has ceased.

Further investigation of the infrared emission in tritium-doped samples by Magnotta *et al.*<sup>18</sup> showed that optical irradiation at the wavelength of the bound-free bubble transition enhanced the infrared emission. By using a Xe arc lamp and a monochromator fitted with optical long-pass filters the researchers were able to examine the induced emission at 800 nm as a function of the wavelength of incident light. The resulting induced emission was found to maximize when the wavelength of the ultraviolet radiation was at the bound-free maximum (about 330 nm), and decrease as the wavelength of the incident radiation is moved away from this value. The authors use these observations in conjunction with a previously developed square-well model to suggest that the emission is a result of radiative electron localization by lattice defects. The studies on solid DT also observed an 8 nm redshift in the emission as the temperature was raised from 4.5 K to 10 K.

Despite a substantial body of experimental research, the origin of the infrared emission in irradiated solid deuterium remains uncertain. The purpose of the experiments to be presented herein was to investigate some of these more recent developments, especially those dealing with phenomena that occur after proton beam irradiation has ceased. Flashes induced after termination of the proton-beam will be presented. Timing of the post-irradiation continuous emission will also be presented along with its temperature dependence. Studies involving optical irradiation, using both a laser and a Xe arc lamp, will be shown to effect the results only after proton-beam irradiation has ceased. Finally, the effect of induced flashes, after proton-beam irradiation has ceased, on the infrared charge-induced lines will be presented.

## II. EXPERIMENT

In our experiments the sample is irradiated by a beam of 15-MeV protons. Roughly half of this energy is deposited into the solid sample. Beam currents are typically 10 nA, leading to a current density of 10 nA/cm<sup>2</sup>. Proton-beam current is measured by an oscillating grid which intercepts 50% of the incident beam. This enables spectra to be taken in which each channel has a constant charge (and energy) delivered to the sample rather than constant time per channel. This beam current normalizing, which eliminates most noise due to beam current fluctuations, is imperative when studying weak emission features. The sample is contained in a copper cell with interior volume of 0.8 cm<sup>3</sup> which is mounted on the end of a liquid-helium transfer-line cryostat, to which is attached a calibrated silicon diode thermometer. To achieve temperatures below 4.2 K, the exhaust of the transfer line can be pumped by a large rotary pump. The lowest stable temperature attainable within the cell using this system is 2.6 K. The cell temperature has been calibrated below 4.2 K by measuring the equilibrium vapor pressure of helium in the sample cell. The temperature inside the sample while the proton beam is on may be about 0.5 K higher than our quoted values.<sup>4</sup>

The light emitted by the sample is focused onto the entrance slit of a McPherson model-218, 0.3-m scanning monochromator equipped with a 600-l/mm grating blazed for 1  $\mu$ m. The detector is a cooled Hamamatsu R-3310 photomultiplier tube with response out to 1040 nm. Order sorting was accomplished with a 515-nm long-pass filter and a slit width of 1 mm was used for most experiments. This corresponds to a spectral width of 2.7 nm. The signal from the photomultiplier was preamplified and then input to a Stanford Instruments SR-400 photon counter. For timing measurements the monochromator is fixed at one wavelength while scans are acquired as a function of time.

Post-irradiation emission from the solid was studied using two different methods. The first method involved the use of an EG&G model-2100 nitrogen-pumped dye laser with a selection of dyes to cover the spectral region of the ultraviolet spectrum. Since the ultraviolet spectrum is very broad, each dye was only used at its lasing maximum. Laser power was measured by a Newport 1825-C power/energy meter with an 818J-09 energy detector head. Laser energy varied from 16  $\mu$ J/pulse at 365 nm to 35  $\mu$ J/pulse at 425 nm. The pulse rate used was 10 Hz, leading to cw-equivalent powers of 160–350  $\mu$ W. Spectra were acquired both with the proton beam incident on the sample as well as after termination of the irradiation.

Additional studies involved replacing the laser with a Xe arc lamp having a 10-nm bandpass filter centered at 361 nm. This could be used as a comparison to the laser results to see if the short duration of the laser pulse had any effect. Spectrophotometric measurements showed the filter to have  $\sim$ 0.02% transmission at 850 nm. Since these experiments involve passing the ultraviolet beam into the sample and hence to the detector, any infrared light produced by the Xe lamp and transmitted by the filter could easily dominate any induced emission signal. For this reason light from the Xe arc lamp was also passed through 4 cm of saturated  $CuSO_4$  solution. The resulting combination of UV filter and

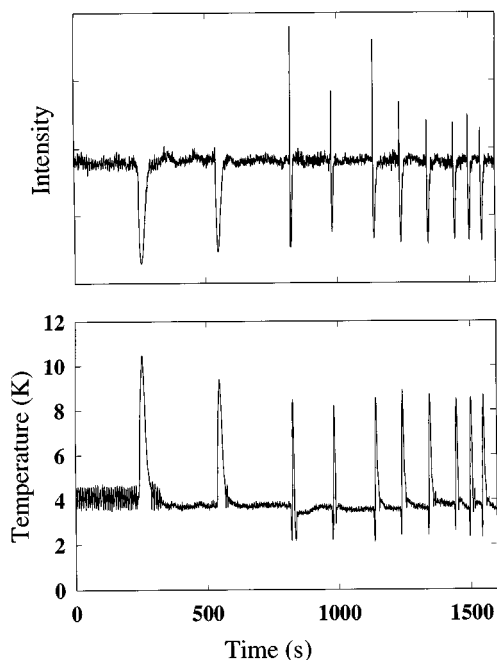


FIG. 1. Temperature changes (bottom) and their effect on the red emission (top).

CUSO<sub>4</sub> solution has a rejection of greater than  $10^8$  through the infrared spectral region of interest while transmitting  $\approx 20\%$  in the 10-nm region centered at 361 nm. Even this large rejection passed a measurable amount of IR signal as will be shown subsequently. For experiments involving the lamp-filter combination an additional long-pass filter is included in the optical path before the PMT to decrease the second-order UV light which allowed us to start our scans as low as 740 nm, below which saturation of the PMT from second order light was still a problem.

### III. RESULTS

#### A. Post-irradiation stimulated flashes

In addition to observing spontaneous optical flashes, reported previously,<sup>16</sup> studies were done on triggered flashes such as those described by Mapoles *et al.*<sup>17</sup> Our studies were not aimed at reproducing the results of Ref. 17 but rather at expanding upon them, especially where differences in the two systems exist. Figure 1 shows a series of attempts at inducing flashes in our experiment. In the first two attempts the temperature was raised simply by increasing the heater voltage from a value required to keep the temperature at 4 K to some larger value. It can be seen that for this case the temperature rises from 4 K to a maximum of almost 9 K quite slowly, taking about 20 data points or 12 s. The top portion of the figure, showing the emission intensity, illustrates the fact that with this thermal stimulus the emission responds to the temperature, becoming weaker as the temperature is raised. Successful attempts at inducing flashes involve a different method of raising the temperature. For these attempts the heater was on with some small current to keep the temperature at 4 K. The temperature was kept at this value since allowing the temperature to drop below 4 K resulted in the occurrence of spontaneous flashes when they

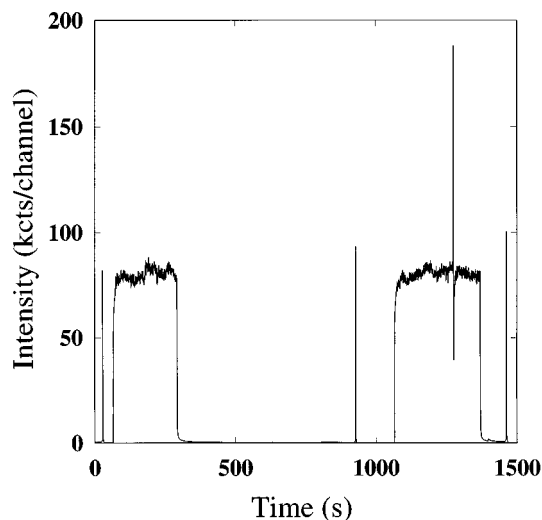


FIG. 2. Emission at 820 nm showing flashes with proton beam off.

were undesired. To induce a flash the leads were briefly disconnected from the heater, the voltage raised to a much larger value, and the leads reconnected for a short time, usually about 1 s. This procedure resulted in a much faster temperature rise. For this latter method the temperature rose to a maximum of just over 8 K in seven data points or about 3 s.

Proton-beam irradiation gives one the option of studying the sample after irradiation has been terminated. It was found that it was indeed possible to induce flashes after the proton beam had been turned off. Figure 2 shows part of a long scan with the proton beam both on and off. At  $t=0$  in this figure the proton beam is off, but had been on for some time previously. Shortly after the beginning of this scan, the first induced flash is observed, confirming the fact that flashes can occur without ionizing radiation being simultaneously present. Inducing flashes after irradiation has ceased is not possible for DT samples. The proton beam is allowed to strike the sample again at  $t \approx 100$  s. The increased count rate is the steady-state emission described previously.<sup>15</sup> After about 150 s of irradiation the beam is turned off once more. A second flash is induced at  $t \approx 900$  s. This time is greater than 10 min after the sample irradiation was stopped. At  $t \approx 1100$  s irradiation is resumed, and during this period a spontaneous flash is observed. The beam is turned off and one final post-irradiation flash is induced at  $t \approx 1400$  s. There are two important observations concerning this figure. First it is obvious that the induced flashes have about the same integrated intensity as the one spontaneous flash (since the time for an optical flash is less than the channel dwell time, the integrated intensity of the flash is just the value of the one point above the base level). In addition one can see that it is possible to induce a flash over 10 min after termination of irradiation. (In a later run, we were able to induce a flash 60 min after termination of irradiation.) The resulting flash also has the same integrated intensity as the other flashes in the figure. The pulse shape of flashes induced after the irradiation was terminated was also investigated. Both the turn-on and turn-off of the induced flashes are similar to those of flashes induced while the beam is on the sample.

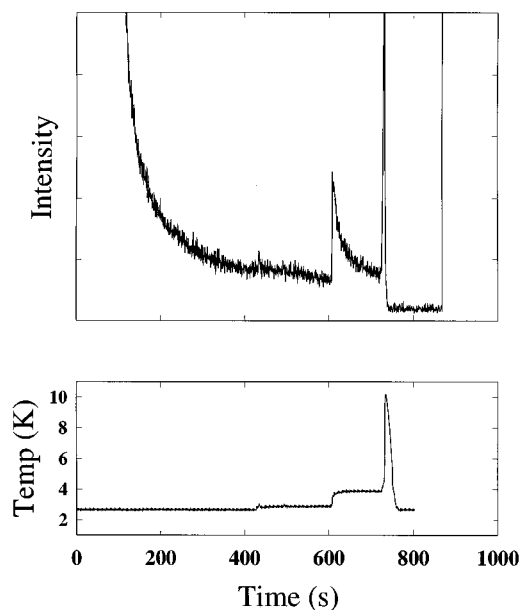


FIG. 3. Emission from central portion of Fig. 2 (300–1100 s) using a more sensitive vertical scale (top). Sample temperature recorded at the same time (bottom).

### B. Emission decay

Figure 3 is a blow up of Fig. 2 both before and after the stimulated flash that occurred 10 min after termination of radiation. The lower part of the figure shows the temperature. The proton beam was turned off at 100 s. Some heat was applied to the heater just after 400 s and more was applied at 600 s. Three things are noteworthy in this figure. The first is that while the emission intensity drops sharply (90% decrease in less than 1 s) there is a residual emission that persists for minutes after the proton beam has been turned off. The second point is that the emission intensity increases with increasing temperature after irradiation has ceased while we previously observed that it decreases with increasing temperature during irradiation. And finally note that following the induced flash the residual emission is quenched; the count rate is only equal to the dark count of the detector.

Emission decay curves were acquired at wavelengths of 720, 820, and 920 nm and were analyzed using standard nonlinear regression of multiexponentials. In all instances the curves could be well fit having a residual intensity given only by the detector dark count. At 4 K, the intensity decayed faster at the lower wavelengths than at the higher. We are most interested in how long it takes for emission to cease. For instance, at 720 nm, the longest-lived component, with an amplitude fraction of 1.9%, has a lifetime of  $80 \pm 8$  s. At 920 nm, however, the longest-lived component, with an amplitude fraction of 0.6%, has a lifetime of  $756 \pm 130$  s. The 820-nm data set is intermediate with a value of  $278 \pm 13$  s and an amplitude fraction of 0.4%. Comparisons of all of the lifetimes among the three wavelengths show no common values, a situation indicative of a nonexponential decay. Goodness-of-fit tests are inconclusive, and so the use of multiexponential analysis to obtain some estimate of the time frame of decay seems reasonable.

A simple radiative reaction is not expected to result in a wavelength dependence to the decay times of the beam-off

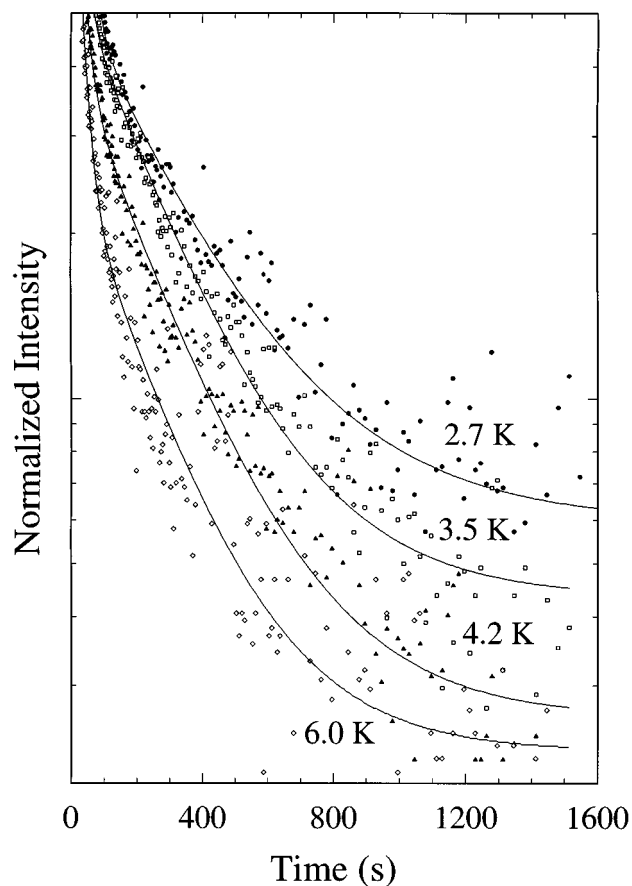


FIG. 4. Emission decays at 860 nm at 2.7 K (circles), 3.5 K (squares), 4.2 K (triangles), and 6.0 K (diamonds).

intensity of this red emission feature. However, we have reported that there is a wavelength shift of the peak of the emission as the temperature is raised and also that the wavelength of the maximum of the flash intensity is different from the wavelength of the maximum of the continuous red emission intensity at the lowest temperature measured.<sup>13</sup> The present result, along with those, argues that at least two different mechanisms or perhaps two different species are involved in these emission phenomena.

We were also able to measure emission lifetimes at a wavelength of 860 nm for four temperatures from 2.7 to 6.0 K. The long-lived tails of these decay curves are plotted on a semilogarithmic scale in Fig. 4. The data have been normalized to their peak intensities and the dark count has been subtracted. That the decays are faster at the warmer temperatures is consistent with all radiation-induced effects measured thus far.

### C. Ultraviolet-induced emission

The proton-irradiated samples were also studied while under irradiation by ultraviolet light from a nitrogen-pumped dye laser exciting the electron bound-free spectrum. Previous studies in DT samples showed that with  $90 \mu\text{W}$  of incident ultraviolet radiation near the UV absorption maximum, the IR emission signal rose by a factor of 2. In contrast, our studies were not able to discern any difference in the infrared emission while the laser light was incident on the sample at the same time the proton beam was on. Our experimental

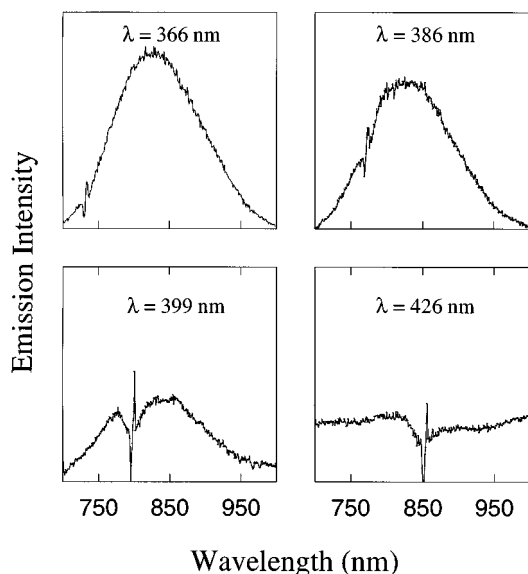


FIG. 5. Laser-induced emission spectra following proton-beam irradiation but taken with the proton beam off at four different laser wavelengths.

technique, however, allows us to acquire spectra with the ultraviolet light striking the sample, but the proton beam intercepted before the sample. The electron bubble concentration is known to decay in about 20 min after termination of the proton beam and this lifetime is not significantly shortened by exposure of the sample to ultraviolet laser light.<sup>7</sup> Hence, the electrons that are “detrapped” by the UV light are replaced before the lattice relaxes to fill in the bubble. Under these conditions we observed that the ultraviolet radiation from our laser induced an emission identical to the low-temperature infrared emission as shown in Fig. 5. The spectra in Fig. 5 have had the laser background subtracted, and the sharp peaks at the second-order laser line positions are a result of this normalization. The induced emission shown in the figure represents  $\approx 10\%$  of the proton beam-on value. If the emission feature results directly from a radiative process involving the electrons as the previous data suggest,

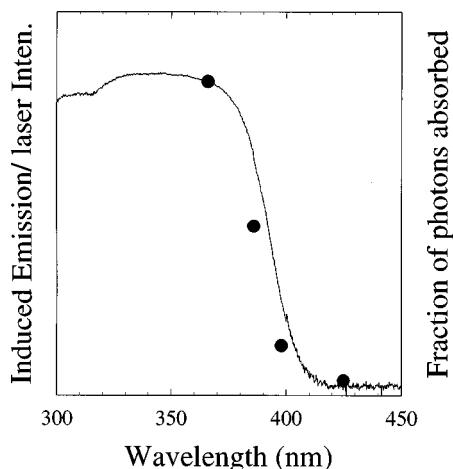


FIG. 6. Absorption intensity of proton-irradiated solid  $D_2$  (curve) and stimulated, normalized emission intensity (circles). The circle at 366 nm has been placed on the curve for comparison purposes.

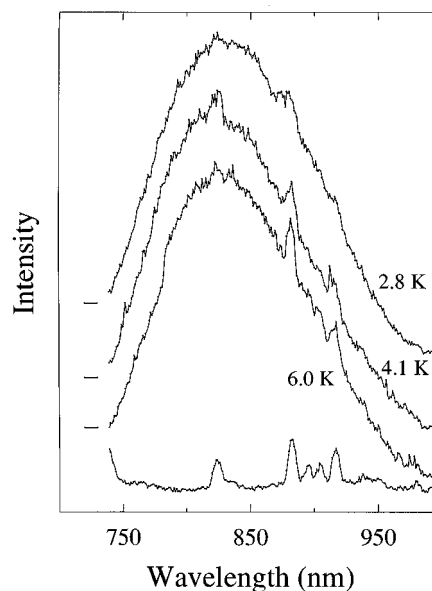


FIG. 7. Xe arc lamp induced emission spectra following proton-beam irradiation at a selection of temperatures. The unlabeled curve is residual lamp intensity through the same sample prior to proton-beam irradiation.

then the induced emission must be proportional to the number of electrons ejected from their traps and, hence, to the number of photons absorbed.

Figure 6 shows the induced emission as a function of UV excitation wavelength. The induced emission has been normalized to the incident laser power. The figure also shows the UV absorption spectrum as measured by Forrest *et al.*<sup>7</sup> The agreement is excellent, and we can conclude that as in Ref. 18, pumping the UV absorption feature leads to an enhanced infrared emission. While the result described above is qualitatively the same as that described for DT samples,<sup>18</sup> the difference in intensity should be noted. At an excitation wavelength of 365 nm the induced effect is small enough that it cannot be discerned when the proton beam is incident on the sample. The cw-equivalent laser power in our case is  $\approx 130 \mu\text{W}$ , which is greater than (but comparable to) the power described by Magnotta *et al.*<sup>18</sup> Since it is plausible that the very short ( $\approx 1$  ns) pulse width of the laser could have some effect, the induced emission was also studied using a Xe arc lamp. With a 150-W lamp similar to that described in Ref. 18 we were able to obtain  $\approx 12 \mu\text{W}$  of UV power. This power is an order of magnitude less than that used in laser studies, but gives a comparable value for the induced emission. This suggests that the laser light saturates the absorption transition.

Induced spectra using the Xe arc lamp as the UV light source are very similar to the first spectrum in Fig. 5, and also to the low-temperature red emission. With this experimental arrangement, induced infrared emission spectra were acquired at 2.8 K, 4.1 K, and 6 K which are shown in Fig. 7. The proton beam had been on the sample for some time prior to both the 2.8-K and 4.1-K curves but the curves are taken with the proton beam off. In fact the 6.0-K curve was taken immediately after the 4.1-K curve with no additional proton-beam irradiation taking place. The unlabeled spectrum at the bottom of the graph is the residual lamp intensity passing through the same sample of solid  $D_2$  before being irradiated

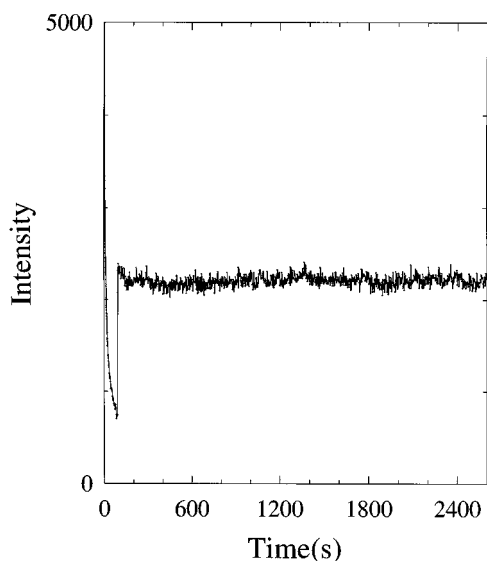


FIG. 8. Xe arc lamp induced emission intensity at 820 nm and 2.8 K as a function of time.

with protons. The 6-K spectrum is plotted with the same origin as the residual lamp spectrum and the vertical scale is linear. The 4.1-K and 2.8-K spectra have each been displaced vertically by the amount indicated by the small horizontal line at the left of the curves for clarity of presentation. Without such displacement the three curves would almost lie on top of each other, demonstrating a particularly weak temperature dependence. Only the sharp spectral features observed by Momose *et al.*<sup>19</sup> in gamma-irradiated solid parahydrogen have shown such insensitivity to temperature increases.

The timing behavior of the UV-induced IR emission was studied by irradiating the sample with the proton beam, terminating the radiation, and then illuminating the sample with UV radiation. One such curve is presented in Fig. 8, taken at 820 nm and 2.8 K. The intensity is the number of photon counts in 0.5 s. With the proton beam on, the emission intensity was 124 000 counts and the beam was turned off at time 0. The decay curve seen at the start of the plot would be similar to the one on Fig. 4. After turning off the proton beam, we had to walk into the target room to rotate a shutter, thereby illuminating the sample. This illumination started 92 s after the proton beam was turned off. The extraordinary result presented here is that the emission intensity shows no decrease for over 40 min. Curves were also acquired at 4.1 and 6.0 K with only the warmer one showing a slight decrease in intensity (lifetime  $\tau=5500$  s). The intensities of these curves were nearly the same, consistent with the spectra of Fig. 7. The timing is also consistent with Fig. 7 if one reflects that the 6.0-K curve of that figure was started 20 min after the start of the 4.1-K curve with no intervening proton-beam irradiation.

#### D. Infrared absorption features

Unambiguous signatures of charge-induced species occur in the infrared spectral region, around  $3 \mu\text{m}$  for deuterium. These have been described previously<sup>2,3</sup> and represent Stark-shifted absorption lines caused by a positive ion cluster (the  $Q_1^+$ ) and an electron bubble (the  $Q_1^-$ ). We had previously

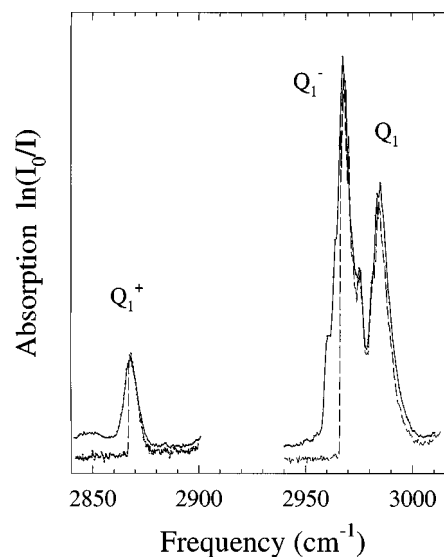


FIG. 9. Charge-induced IR absorption features during proton-beam irradiation (smooth curve); same spectrum with proton beam terminated and flash stimulated while spectrum positioned at peak of absorption (dashed curve).

taken data during proton-beam irradiation that indicated that following a spontaneous or induced flash the intensities of these infrared charge-induced features were substantially reduced.<sup>20</sup> However, these features persist for some time following termination of the beam and we wanted to learn whether they would disappear if a flash were induced after proton-beam irradiation had ceased.

We performed this experiment two ways. With the spectrometer tuned to the spectral feature of interest we monitored the lamp intensity for an annealed sample and then turned on the proton beam and watched the absorption feature grow in. After several minutes of irradiation we terminated the proton beam, stimulated a flash (as monitored by the temperature), and observed the resultant lamp intensity. In each instance the intensity immediately returned to its preirradiation value.

The second way of doing the experiment is illustrated in Fig. 9. The solid curve represents beam-on spectra over the wavelength range of interest. The dashed curves were acquired separately for each part of the figure. The beam was on as the spectrum scanned up in *wavelength*. At the peak of the  $Q_1^-$  line, the proton beam was turned off and a flash was stimulated as the scan continued. This was repeated for the  $Q_1^+$  line. One can see quite clearly that there is no observable intensity remaining to the charge-induced features following a flash. Whether this should be attributed to anything more than heating associated with the flash will be discussed below.

The time frame for transparency following a flash was measured to be 73 ms for the  $Q_1^+$  line and 85 ms for the  $Q_1^-$ .<sup>20</sup> Given that the decay curves were well fit with single exponentials, and the uncertainties are about 10 ms, we take the lifetimes for the two features to be the same. This is in marked contrast to the long but disparate lifetimes (minutes to hours) measured for these features after termination of the proton beam.<sup>4</sup>

## IV. DISCUSSION

### A. Summary of observations

While the main thrust of this paper is to present those results occurring in solid deuterium after termination of the proton beam, it was hoped that by doing these experiments we would be able to present a coherent picture of *all* of the emission phenomena from proton-irradiated solid deuterium. We would like to summarize the principal results that need to be explained here, giving reference to the original literature for those points not presented in this paper.

(1) A continuous red emission spectrum is observed during proton-beam irradiation of  $D_2$  maximizing near 830 nm.<sup>15</sup> The emission becomes weaker as the temperature is raised but is still measurable at 17.4 K, persisting to higher temperatures than other charge-induced features.<sup>13</sup> We have observed the same spectrum in  $H_2$  with a much weaker intensity.

(2) After tens of minutes of proton-beam irradiation at 2.6 K, spontaneous optical flashes occur with a spectrum similar to the continuous emission but redshifted by about 100 nm. The flash frequency increases with duration of irradiation, becoming about one flash per minute after 2–4 h. The flash frequency is also a sensitive function of sample temperature becoming less frequent as the temperature is raised and essentially not occurring at temperatures above 4.2 K.<sup>16</sup>

(3) Both the amplitude and time frame of bleaching of the steady-state emission following a flash are wavelength dependent.<sup>16</sup>

(4) It is possible to stimulate a flash tens of minutes after proton-beam irradiation has ceased.

(5) When the proton beam is on, the continuous red emission decreases in intensity as the temperature is raised, but when the proton beam is off, the weak residual emission increases in intensity as the temperature is raised (Fig. 3).

(6) After proton-beam irradiation has ceased, the continuous red emission shows a long-lived component whose lifetime is wavelength dependent and whose intensity is quenched by an induced flash.

(7) After proton-beam irradiation has ceased, the continuous red emission can be stimulated by UV photons through irradiation by a laser or an arc lamp. The emission intensity tracks the previously measured UV absorption spectrum of irradiated solid  $D_2$ .

(8) This [(7) above] post-irradiation, UV-stimulated, red emission spectrum is insensitive to temperature changes from 2.8 to 6.0 K, and persists for over 30 min with no noticeable decrease in intensity at 2.8 K.

(9) After termination of proton-beam irradiation, the infrared, charge-induced absorption features are quenched following a stimulated or spontaneous flash.<sup>20</sup>

In addition to explaining the items delineated above, we must seek a model consistent with all previously observed charge-induced effects including tritium doping and  $\gamma$ -ray irradiation. That a charge concentration  $> 10^{16} \text{ cm}^{-3}$  exists during proton-beam irradiation along with an atom concentration of  $\sim 10^{19} \text{ cm}^{-3}$  is well established. That flashes observed in these experiments are caused by atom-atom association is accepted, based mostly on the energetics. That the positive ions exist in two or more species, one of which is highly immobile,  $D_n^+$ , while negative charges also exist in

two or more species, one of which is an electron bubble is also well established.<sup>4,13</sup> But the solid hydrogens are both a fundamental and a simple system and we ought to be able to address the details of the myriad of interactions occurring both during and after ionizing radiation strikes the sample.

### B. Proposed models

While it is not difficult to come up with a mechanism that would result in continuous emission between 800 and 900 nm, if one considers that the flash spectrum, is the same as the continuous spectrum, then one needs a mechanism that in some way can be related to atom-atom association. However, while atoms are formed during ionizing radiation, few if any will be formed after such radiation ceases. Nevertheless, the continuous emission persists under certain circumstances for tens of minutes after irradiation (see Figs. 4 and 8). If atom-atom association were responsible for this emission, the atom numbers would become rapidly depleted and the occurrence of a flash 1 h after termination of radiation would not be possible.

Clearly mobile electrons play a leading role in all of the phenomena considered here. We take the results of Fig. 6 to unmistakably link the continuous red emission to electrons that have been detrapped after termination of ionizing radiation. And here lies one of the largest difficulties. The electron bubbles are known to decay in number over a time frame of tens of minutes.<sup>4</sup> How is it that UV radiation can stimulate a cycle of red emission that shows no decay over 30 min?

The reader must recall that atom-atom association for hydrogen has a vanishingly small cross section when the atoms are in their ground state even though the process is energetically highly favored because there is no way to get rid of the excess energy. (Radiation between vibrational levels of the ground-state potential is forbidden since a homonuclear molecule has no dipole moment.) In the solid, this argument is weakened because quadrupole moments on adjacent molecules can induce a dipole on the colliding pair but such induced dipoles are weak and we propose that such a mechanism is not of primary importance in our samples.

The scenario that seems to fit most (but not all) of the observations is radiative electron attachment to unpaired atoms. This process has been observed in shocked gas tubes with hydrogen. The electron temperatures for those experiments was of the order of 10 000 K, with densities of the order  $10^{16} \text{ cm}^{-3}$ . Radiative attachment of electrons to hydrogenic atoms has a very low cross section, and requires systems with large concentrations of unpaired atoms and electrons. Traditional gas discharges do not have such large concentrations of atoms, but the conditions in our sample cell are ideal for observation of such a process. The atom concentrations in these solids is  $\approx 10^{19} \text{ cm}^{-3}$  and the concentration of trapped electrons is  $\approx 10^{16} \text{ cm}^{-3}$ . The small polaron concentration is thought to be perhaps an order of magnitude larger than this. The inverse process of photodetachment of hydrogen negative ions is well studied, and the absorption spectrum for this process is very similar in both position and structure to the infrared emission.

The idea that  $D^-$  formation causes the continuous red emission becomes more appealing when one realizes that there are at least two channels available to this negative ion. If it is close to a neutral atom, association will occur with a large cross section releasing the electron. If it is close to a lattice defect or a site from which an electron was recently ejected from a bubble, then the electron could detach from the ion reoccupying the bubble. This mechanism provides a cycle that might explain the result of Fig. 8.

There is now some direct and indirect evidence that electron bubbles are not the only immobile negative charge center in irradiated solid hydrogens and may not even be the most robust. A recent ESR experiment by Miyazaki *et al.*<sup>21</sup> has been interpreted by Symons<sup>22</sup> as evidence for  $H_2^-$  in solid irradiated hydrogen. This molecular ion is not stable in vacuum and, if the interpretation is correct, must be stabilized by the solid. This would involve the formation of a local environment, perhaps caused by a lattice defect or vacancy, to change the energetics enough for the electron to localize around a single molecule and furthermore for this electron to be highly immobile. It would have to be smaller and less mobile than a small polaron, many of which are certainly present during ionization. Indirect evidence for the existence of such an entity is provided by the work of Momose *et al.*<sup>19</sup> Both Miyazaki and Morikita and Momose *et al.* use  $\gamma$ -ray irradiation of solid hydrogen, performing their experiments hours after radiation has ceased. While earlier proton-beam irradiation experiments gave evidence that charges could exist in solid deuterium for tens of minutes after irradiation had ceased, we have never had direct evidence, in the form of charge-induced spectral features, of charges persisting to temperatures just under the melting point. Such negative charges, proposed by Momose *et al.*,<sup>19</sup> must exist at concentrations too low to be detected in our experiments. But it is precisely such charges that could be liberated by UV photons, take part in radiative recombination with an atom, and return to a suitable deformity in the solid. The energetics of such charges have not been worked out but they must be the same as the electron bubble state for this interpretation to work.

The idea, then, is that some significant number of positive ion clusters, negative bubbles or  $D_2^-$ , and atoms persists for long times after ionizing radiation has ceased. The number densities for the charged species have to be at least  $10^{-2}$  lower after than during irradiation and can be approximated by the number density of positive ion clusters, about  $5 \times 10^{14} \text{ cm}^{-3}$ .<sup>4</sup> Atom densities have been estimated to be  $10^{19} \text{ cm}^{-3}$  during irradiation such that in a steady state about 1% of them recombine during a flash which occurs about every minute.<sup>20</sup> In our experiment the atom density after termination of radiation has not been measured but we assume it is significantly higher than the ion concentration. Because there is no reason to consider a stimulated flash to be qualitatively different from a spontaneous one, and atom densities must be in excess of  $\sim 10^{18} \text{ cm}^{-3}$  for the first flash to spontaneously occur, we expect the post-irradiation atom concentration to be  $> 10^{18} \text{ cm}^{-3}$ .

If radiative attachment is the mechanism for the red emission, and atom-atom association proceeds via  $D^-$ , then a flash can occur whenever association takes place before the

electron detaches to a lower-energy bound state (bubble or  $D_2^-$  complex). A sufficiently high atom concentration is needed before an atom is close enough to a  $D^-$  for this reaction to proceed. Once it occurs, the energy released warms the local medium, increasing the diffusion rate of atoms, allowing more to react, and a chain reaction ensues. Once the concentration is lowered a bit (by about 1%) the reaction ceases.

If one expands the core idea to say that the red emission is caused by radiative localization of the electron which cannot only proceed via atoms but can also proceed via vacancies,  $D_2$ , etc., which may in fact be dominant during proton irradiation, then most observations can be accommodated. This mechanism was first proposed by Magnotta *et al.*<sup>18</sup> Such electrons could scatter back into the continuum during proton-beam irradiation before forming an electron bubble. This could explain why the continuous red emission reaches its maximum intensity in less than 1 min of ionizing radiation while the bubble related charge-induced effects take several minutes to maximize. It could also explain the wavelength dependence noted in items (3) and (6) of the summary.

One item left to explain is that flashes can be stimulated tens of minutes after irradiation has ceased. The heat pulse given for stimulation increases the mobility of all species, allowing atoms to encounter  $D^-$  ions before the electron detaches. The atom association ejects a fast electron which can itself detrap some localized electron, thereby multiplying by 2 the number of electrons taking part in the reaction. With the proton beam on, there is no problem. If our current interpretation is correct, there must be a significant residual concentration of  $D^-$  ions, or some cluster involving a  $D^-$ , some time after turning off the proton beam.

As alluded to previously, we have had to invoke two different immobile negative charge species and two different radiation mechanisms to begin to explain all of the experimental observations. The two different radiation mechanisms are not energetically that different and so can be used to explain the wavelength dependence of features in the continuous red emission.

## V. CONCLUSION

The outline of a model presented here explains most of the observations and is consistent with previous interpretations of charge-induced effects. However, while there is much in common among the hydrogens there are still notable differences.<sup>23</sup> Mobilities of all species are much higher in hydrogen than in deuterium (at the same temperature), and while the continuous red emission has been observed weakly in hydrogen, no flashes have been observed. Whether such flashes could be seen at lower temperatures is an interesting question. Hence we need to be careful about applying results (such as  $H_2^-$  occurrence) obtained in one isotopomer to another. We consider the large body of experimental evidence now available on the irradiated hydrogens to indicate that the interactions are complex, the number of distinct species is not small, and no simple model is likely to be complete.



## ACKNOWLEDGMENTS

We would like to thank J.L. Hunt, M.F. Svaikauskas, G. Wagner, R. Lamonica, and A. Jirasek for help with datacollection and T. Riddols, G. Mulligan, and W. Williams for technical support. This research is supported by the Natural

Sciences and Engineering Research Council of Canada. We are grateful to the Ontario Laser and Lightwave Research Centre (OLLRC) for the loan of the nitrogen-pumped dye laser.

- 
- <sup>1</sup>P.C. Souers *et al.*, Phys. Lett. **77A**, 277 (1980).  
<sup>2</sup>R. L. Brooks *et al.*, Phys. Rev. Lett. **51**, 1077 (1983).  
<sup>3</sup>R.L. Brooks and J.L. Hunt, Phys. Can. **47**, 132 (1991).  
<sup>4</sup>R.L. Brooks *et al.*, Phys. Rev. B **32**, 2478 (1985).  
<sup>5</sup>J.D. Poll, J.L. Hunt, P.C. Souers, E.M. Fearon, R.T. Tsugawa, J.H. Richardson, and G.H. Smith, Phys. Rev. A **28**, 3147 (1983).  
<sup>6</sup>M.A. Selen *et al.*, Nucl. Instrum. Methods Phys. Res. B **230**, 720 (1984).  
<sup>7</sup>J.A. Forrest, J.L. Hunt, and R.L. Brooks, Can. J. Phys. **68**, 1247 (1990).  
<sup>8</sup>S.K. Bose and J.D. Poll, Can. J. Phys. **63**, 1105 (1985); **65**, 67 (1987).  
<sup>9</sup>R.W.H. Webeler, J. Chem. Phys. **64**, 2253 (1976).  
<sup>10</sup>T. Miyazaki and H. Morikita, Bull. Chem. Soc. Jpn. **66**, 2409 (1993), and references cited therein.  
<sup>11</sup>G.W. Collins *et al.*, Phys. Rev. Lett. **65**, 444 (1990).  
<sup>12</sup>A.S. Iskovskikh, A.Ya. Katunin, I.I. Lukashovich, V.V. Sklyarevskil, V.V. Suraev, V.V. Filippov, N.I. Filippov, and V.A. Shevtsov, Sov. Phys. JETP **64**, 1085 (1986).  
<sup>13</sup>R.L. Brooks, J.A. Forrest, and J.L. Hunt, in *Collision- and Interaction-induced Spectroscopy*, edited by G.C. Tabisz and M. N. Neuman (Kluwer, Dordrecht, 1995).  
<sup>14</sup>B. Stenum, J. Schou, H. Sørensen, and P. Gürtler, J. Chem. Phys. **98**, 126 (1993).  
<sup>15</sup>J.A. Forrest *et al.*, Phys. Rev. B **46**, 13 820 (1992).  
<sup>16</sup>J.A. Forrest, R.L. Brooks, and J.L. Hunt, Phys. Rev. B **50**, 9573 (1994).  
<sup>17</sup>E.R. Mapoles, F. Magnotta, G.W. Collins, and P.C. Souers, Phys. Rev. B **41**, 11 653 (1990).  
<sup>18</sup>F. Magnotta, G.W. Collins, and E.R. Mapoles, Phys. Rev. B **49**, 11 817 (1994).  
<sup>19</sup>T. Momose, K.E. Kerr, C.M. Gabrys, D.P. Weliky, R.M. Dickson, and T. Oka, J. Chem. Phys. **100**, 7840 (1994).  
<sup>20</sup>James A. Forrest, Ph.D. thesis, University of Guelph, 1994.  
<sup>21</sup>T. Miyazaki, K. Yamamoto, and Y. Aratono, Chem. Phys. Lett. **232**, 229 (1995).  
<sup>22</sup>M.C.R. Symons, Chem. Phys. Lett. **247**, 607 (1995).  
<sup>23</sup>J.J. Miller, R.L. Brooks, and J.L. Hunt, Can. J. Phys. **71**, 501 (1993).